SHELL-GROWTH IN RECENT TEREBRATULOID BRACHIOPODA

by DANIEL B. SASS and EUGENE A. MONROE

ABSTRACT. The structure of the brachial valve of four Recent species of terebratuloids was investigated by techniques involving both electron microscopy and light microscopy. The combined approach reaffirmed the conclusions of some previous workers and provided new data on shell growth.

The interpretation of patterns observed when sections are cut through the shells is complicated not only by the spatial orientation of the section itself, but by the habit of the truncated crystals as well. Changes in the nature of crystal growth, orientation, and distribution are shown to be related to retraction of the mantle evidenced at major growth-lines.

CARPENTER (1853) and his contemporaries established the principles upon which succeeding investigations of brachiopod morphology were based. The thoroughness of these pioneer workers and the exotic nature of Recent Brachiopoda did not encourage subsequent detailed research on living representatives of the phylum. According to Williams (1956), less than fifty papers on living brachiopods had been published from the turn of this century to 1956.

This is the second of a series of investigations directed toward a better understanding of the shell structure of Recent Brachiopoda and ultimately, their Paleozoic progenitors. The study was motivated by the published remarks of Muir-Wood (1955, p. 49) and Williams (1956) who stated the need for such an investigation, and the introduction of new techniques which opened areas of search unavailable to earlier workers. The results reported below represent a concordance between the older established approaches and the newer techniques, one complementing the other.

Aknowledgements. Much of the experimental work was performed by the senior author while on sabbatical leave at the University College of Swansea (Glamorgan), Wales. Sincere appreciation is expressed to Professor F. H. T. Rhodes, University College of Swansea, his faculty and staff, for the use of the facilities and the professional courtesies extended. The Department of Metallurgy at Swansea generously provided the use of their electron microscope; Mr. Malcolm Williams was a most valuable assistant during this phase of the research. Discussions with Dr. M. J. S. Rudwick, Dr. H. Brunton, and Mr. E. Owen were helpful in framing experimental procedures and interpreting results. Mr. S. Osborne of the Geology Department, Swansea, produced the photographs used in this report.

Materials and methods. Four species of Recent terebratuloid brachiopods were especially examined; *Gryphus stearnsi* (Dall and Pilsbury 1891), *Pictothyris picta* (Dillwyn 1817), *Laqueus californicus* (Koch 1848), and *Terebratalia transversa* (Sowerby 1846). The discussions which follow are collective in nature with reference made to individual species as required. Specific references to *G. stearnsi* and *L. californicus* occur frequently in the text due to the superior nature of the preparations made from these shells, for they lent themselves more readily to the techniques employed.

The two-step plastic–carbon method of replication employed in the electron microscopy, was essentially as reported by Sass *et al.* (1965, p. 181). Observations and photographs were made on an AEI model EM6. Electron micrographs taken of trans-

[Palaeontology, Vol. 10, Part 2, 1967, pp. 298–306, pls. 44–49.]

verse and longitudinal sections were overlapped and assembled as mosaics for the study of gross morphology (Pl. 44, 45). Specimens studied by light microscopy were prepared, with some modification, in a manner originally described by Carpenter (1853). Fragments of the predominantly calcite shells were treated for 6 hours at 50° C in 30 per cent. H_2O_2 to oxidize the trace organic constituents. Some portions of oxidized shell fragments were carefully exfoliated and the component parts studied separately with a binocular microscope; other portions were disaggregated ultrasonically and observed with a polarizing microscope.

To establish a standard for the comparison of results, all preparations were made from the brachial valves of the species enumerated above. Replications for longitudinal sections were made from faces cut along the plane of symmetry of the valve. Transverse sections were prepared from faces cut perpendicular to the plane of symmetry at the maximum width of the valve. Tangential sections were taken at various levels reached by repeated controlled abrasion and etching from the surface downward at the intersection of the two planes.

All registration numbers refer to the collection stored in the Department of Geology at Alfred University, Alfred, New York. The replications from which electron micrographs were made are preserved together with the shell material under the same number.

SHELL MORPHOLOGY

Sass *et al.* (1965), considered the brachiopod shell to consist of four distinct components; the periostracum, outer carbonate layer, inner carbonate layer, and adventitious layer. The terminology applied was selected from a variety of names then in use. To avoid an unnecessary proliferation of terms the writers have adopted herein the terminology of Williams and Rowell (1965). Reference to the shell components mentioned above, subsequently appear respectively as the periostracum, primary, secondary, and prismatic layers.

Periostracum. It was not possible to study the periostracum although its presence was noted on some of the specimens in the writers' collection. The techniques used in preparation were either unsuitable or destructive. Its origin and characteristics are documented by Williams (1956, p. 244); his conclusions will be discussed elsewhere in this paper.

The primary layer. In previous work devoted exclusively to electron microscopy the writers were unable to obtain satisfactory photographs or data on this portion of the shell. Our subsequent efforts have been more successful in obtaining evidence of some of its characteristics, but detailed interpretation remains tenuous. The constituent calcite crystals of the layer have been characterized as 'fibrous' by Cloud (1942, p. 23) for the Recent species *L. californicus* (Koch) and as 'lamellar' by Dunlop (1961, pl. 483) for the Carboniferous species *Spirifer trigonalis* (Martin). Cloud (1942, p. 24) suggested that the fibres are oriented vertically with respect to the shell surface and that their crystallographic *c* axes are parallel to the length of the fibres.

The primary layer is easily differentiated from the succeeding secondary layer at both high (Pl. 44, 45) and low magnifications (Pl. 48, fig. 1). Replications of etched surfaces viewed at high magnifications and various orientations give somewhat conflicting impressions of the three-dimensional structure. The etched upper surface of the layer

(Pl. 47, fig. 6) has a pock-marked appearance which could be derived from tightly packed prisms with their long axes oriented perpendicular to the shell surface. An enlargement of an etched longitudinal section (Pl. 46, fig. 2) suggests a lamellar structure. Further enlargement of a transverse section at $\times 10{,}000$ (Pl. 46, fig. 3) showed a peculiar nodular structure, the interpretation of which is not clear. Efforts to disaggregate the layer into its component crystals by ultrasonic vibration have so far been unsuccessful. If the microstructure of the layer conforms to the observations of Cloud, cited above, the accommodation of the caeca must be accomplished by the clustering of the crystals around each individual caecum to form the puncta. The inflation of the distal end of the caeca, when traversing the primary layer, is a phenomenon which has been well documented but rarely shown photographically (see Cloud 1942, pl. 2, fig. 1). Replications of this characteristic were fortuitously made on two occasions during this study. The nature of the inflation is apparently unique for each species as the electron micrographs of *G. stearnsi* (Pl. 46, fig. 1) and *P. picta* (Pl. 46, fig. 4) suggest.

Studies of exfoliated material at lower magnifications yield additional information about the primary layer. The layer is relatively uniform in thickness and compact. Its outer surface is marked by concentric growth-lines some of which are more heavily incised than others (Pl. 48, fig. 1). The underside of the layer (Pl. 48, fig. 2) reflects only the more heavily incised growth lines and reveals that the punctae themselves may vary considerably in both size and shape.

EXPLANATION OF PLATE 44

All sections are composite electron micrographs of the brachial valves. Orientation with the valve exterior uppermost.

Figs. 1–2. *Gryphus stearnsi* (Dall and Pilsbury 1891). Tosa, Japan. 1, Longitudinal section showing primary, secondary, and prismatic layers. Crystals of the prismatic layer, accentuated by etching along cleavage planes, are well displayed on bottom portion of photograph. Alfred Univ. 09130-1A. 2, Transverse section of the same valve. The prismatic layer at the base is interrupted by a repetition of the secondary layer. Alfred Univ. 09130-4B.

Figs. 3–4. *Pictothyris picta* (Dillwyn 1817). Tosa, Japan. 3, Incomplete longitudinal section showing the primary layer and a portion of the secondary layer. Note the increase in crystal size toward the base of the section. Alfred Univ. 09130-1F. 4, Interrupted transverse section showing the primary and upper portion of the secondary layers. The cone-shaped object at the upper right is the mould of the inflated portion of a puncta passing from the secondary to the primary layer. Alfred Univ. 09130-3E.

EXPLANATION OF PLATE 45

All sections are composite electron micrographs of the brachial valve. Orientation with the valve exterior uppermost.

Figs. 1–2. *Laqueus californicus* (Koch 1848). Catalina Island, California. 1, Transverse section showing the primary and a portion of the secondary layer. The club-shaped impression in the centre of the picture marks the passage of the distal end of a puncta. Alfred Univ. 09130-2M. 2, Interrupted and incomplete longitudinal section showing the primary and secondary shell layer. The section is heavily shadowed but accentuates the cleavage of the constituent calcite crystals in the secondary layer. Note the increase in crystal size in the secondary layer. Alfred Univ. 09130-2L.

Figs. 3–4. *Terebratalia transversa* (Sowerby 1846). Puget Sound, Washington. 3, Incomplete and interrupted transverse section, heavily shadowed. The depression along the margins mark the passage of punctae through the secondary layer. Alfred Univ. 09130-1H. 4, Incomplete longitudinal section showing the primary and secondary layers. Note the peculiar pattern of the lower portion of the secondary layer. Alfred Univ. 09130-1G.

1

2

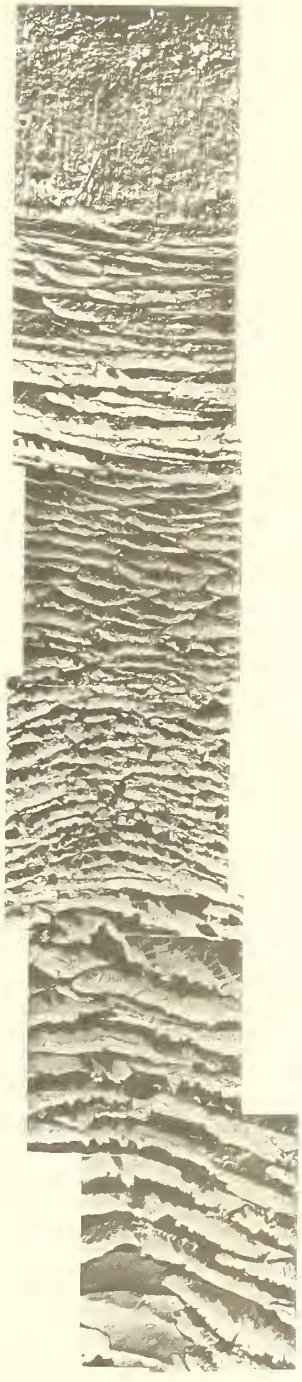

3

4

SASS and MONROE, Terebratuloid shell structures

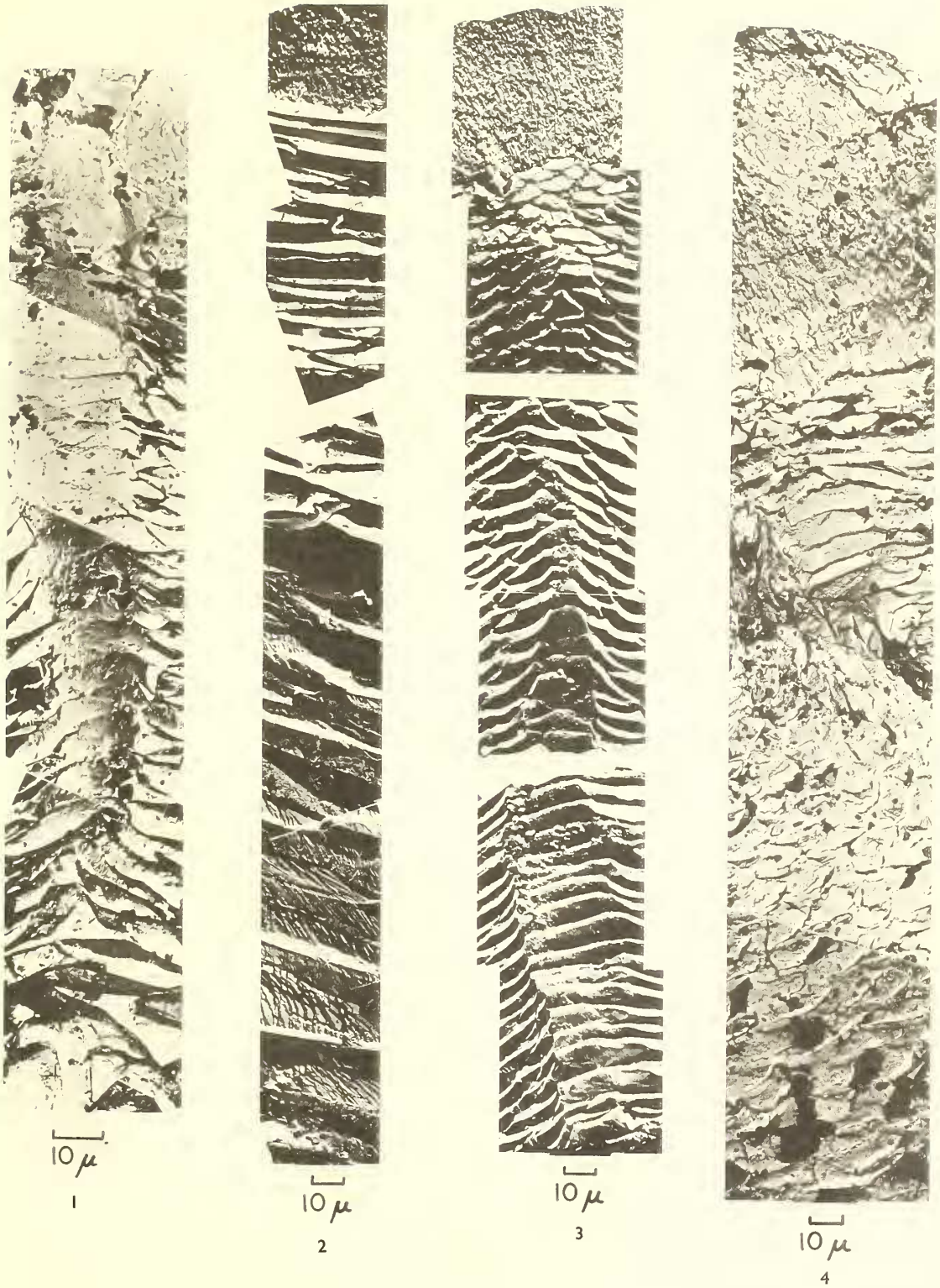

SASS and MONROE, Terebratuloid shell structures

The capacity of the brachiopod to incorporate foreign material within the structure of the primary layer is illustrated on Plate 46, fig. 6. An electron micrograph of one of a number of diatom tests is shown on a tangential section of *L. californicus*. The test was covered by the periostracum and deeply embedded in the primary layer.

The secondary layer. As suggested earlier (Sass *et al.* 1965) the secondary layer appears to vary in character from top to bottom. In longitudinal sections the crystals do show the anterior inclination described by Cloud (1942, p. 24) but the phenomenon becomes less obvious at magnifications above $\times 1000$. Cloud (op. cit.) ascribes the variety of patterns obtainable when viewing thin sections to the angle at which the thin section is cut with respect to the length and width of the shell. The variation in pattern is even more remarkable when seen on electron micrographs (Pl. 44, 45). Because some patterns (Pl. 45, fig. 4) were difficult to interpret in terms of spatial orientation, it was decided to re-examine the material by a different method.

After treatment with H_2O_2, portions of the primary layer of *G. stearnsi* were carefully removed keeping disruption of the secondary layer to a minimum. The ease of separation gave further indication of the sharp junction between the two layers. Viewed with the binocular microscope, the upper portion of the secondary layer consists of a series of bundles of transparent calcite crystals oriented parallel to the long axis of the valve; deviating from this parallelism only as necessitated by the demands of shell curvature (Pl. 48, fig. 1). Crystal growth at this level appears to terminate periodically in conjunction with major growth-lines. Subsequent growth activity may initiate the formation of new independent crystal elements or result in a welding of new increments to the old, causing an inflation at the area of union and producing an arcuate ridge coincident with the major growth-lines (Pl. 48, fig. 3).

Removal of the upper portion of the secondary layer revealed that the intermediate crystalline units below were disposed somewhat differently from those above. They appeared to lie at almost right angles to the long axis of the crystals above (Pl. 48, fig. 1). Careful examination showed that these crystals are deflected toward the shell edges, particularly at major growth-lines, and in extreme cases may recurve posteriorly. Both crystal size and disorder increase as the base of the layer is approached (Pl. 44, fig. 3). The prismatic layer below is frequently approached by a gradational change rather than the abrupt transition which characterizes the contact between the primary and secondary layers.

Tangential electron micrographs of the crystals in the secondary layer (Pl. 46, fig. 5) show the flattened and elongate habit observed by Carpenter (1853) and Cloud (1942). Since the high magnifications were prohibitive for examinations of gross crystal morphology, petrographic and X-ray studies were made of individual crystals separated ultrasonically from oxidized material. X-ray diffraction confirmed that the crystals are composed of calcite, rather than aragonite.

The individual crystals are long with flattened faces; at the juncture of two faces a distinct ridge is formed. Traced along the length of the crystals the ridge exhibits a twist. In addition to twisting, the crystals are curved (Pl. 49, fig. 1) or kinked along their entire length (Pl. 49, fig. 2). The width of the crystals may range from 5 to 15 μ. Measurements of length are difficult to assess since the disaggregation process tends to fragment the crystals. The longest crystal observed measured about 600 μ. Where disaggregation

was incomplete, the crystals are bundled together in a subparallel orientation. The crystals twist about one another with flattening caused by contact. Ridges form along lines where three or more crystals join.

The punctae appear as circular perforations completely within individual crystals or semicircular indentations at crystal boundaries (Pl. 49, fig. 2). Presumably the caeca are accommodated by either individual crystals or aggregates of crystals. In the latter case, an individual puncta or a part thereof is the product of the welding together of the arcuate indentations of two or more crystals. Details of the process are well illustrated at higher magnifications (Pl. 47, figs. 3, 4, 5).

The optical directions, as inferred from extinction under crossed nicols are, in general, inclined to the length of the crystals with the angle of inclination variable from crystal to crystal. Since these optical directions indicate positions of the crystal axis, the axis must also have a variable orientation with respect to crystal length. Thus, the long axes of the crystals are not rational crystallographic directions. This conclusion is surprising in that in the case of inorganic crystals, elongation occurs along a rational crystallographic direction, e.g. a crystallographic axis. It appears that the crystals composing the shell have their morphology determined by environmental conditions, that is, by the organism rather than the physiochemical process of crystal growth.

The prismatic layer. The prismatic layer is usually quite distinct, particularly when viewed at high magnification (Pl. 44, fig. 1). Its component crystals are considerably

EXPLANATION OF PLATE 46

All illustrations are electron micrographs of the brachial valve.

Figs. 1–3. *Gryphus stearnsi* (Dall and Pilsbury 1891). Tosa, Japan. 1, The inflated portion of the distal end of a puncta in a longitudinal section of the primary layer, ×1,500. Alfred Univ. 09130-1A. 2, Enlargement of a portion of transverse section of the primary layer, ×8,000. Alfred Univ. 09130-3C. 3, Enlargement of a longitudinal section of the primary layer, ×10,000.

Fig. 4. *Pictothyris picta* (Dillwyn 1817). Tosa, Japan. The inflated portion of the distal end of a puncta in a transverse section of the primary layer, ×1,500. Alfred Univ. 09130-3E.

Fig. 5. *Terebratalia transversa* (Sowerby 1846). Puget Sound, Washington. Tangential section of the secondary layer showing the disposition of the constituent calcite crystals, ×2,500. Alfred Univ. 09130-1T.

Fig. 6. *Laqueus californicus* (Koch 1848). Catalina Island, California. Tangential section of the primary layer showing the incorporation of a diatom test in the calcite matrix, ×8,000. Alfred Univ. 09130-1Q.

EXPLANATION OF PLATE 47

All illustrations are electron micrographs of tangential sections of brachial valves.

Figs. 1–3. *Gryphus stearnsi* (Dall and Pilsbury 1891). Tosa, Japan. 1, Puncta at the top of the secondary layer showing the accommodation for its passage afforded by the curvature of components of the calcite crystals. Vestiges of the primary layer are represented by the darker material at the top of the picture, ×4,000. Alfred Univ. 09130-1P. 2, The passage of a puncta through the crystal boundaries of the prismatic layer, ×4,000. Alfred Univ. 09130-2P. 3, Detail of the accommodation of a puncta within a single crystal of the secondary layer. The centre portion represents the puncta proper and the peripheral material the crystalline complex surrounding it, ×6,000. Alfred Univ. 09130-1P.

Fig. 4. *Laqueus californicus* (Koch 1848). Catalina Island, California. Puncta (centre oval) in a single crystal of the secondary layer, ×2,500. Alfred Univ. 09130-2Q.

Fig. 5. *Terebratalia transversa* (Sowerby 1846). Puget Sound, Washington. Detail of the passage of a puncta through portions of several crystals in the secondary layer, ×2,500. Alfred Univ. 09130-2T.

Fig. 6. *Pictothyris picta* (Dillwyn 1817). Tosa, Japan. Etched outer surface of the primary layer, ×1,500. Alfred Univ. 09130-1R.